

AD-A051 124

AIR FORCE GEOPHYSICS LAB HANSCOM AFB MASS
STUDY OF THE DUAL-INPUT MODE WITH THE AFGL TWO-METER PATH DIFFE--ETC(U)
OCT 77 G A VANASSE, H SAKAI
AFGL-TR-77-0213

F/G 20/6

UNCLASSIFIED

NL

1 OF 1
ADA
051124



END
DATE
FILMED
4 -78
DDC

2

AFGL-TR-77-0213
INSTRUMENTATION PAPERS, NO. 259



AD A051124

Study of the Dual-Input Mode With the AFGL Two-Meter Path Difference Interferometer

GEORGE A. VANASSE
HAJIME SAKAI

4 October 1977

AD No. _____
DDC FILE COPY

Approved for public release; distribution unlimited.

DDC
RECEIVED
MAR 13 1978
B

OPTICAL PHYSICS DIVISION PROJECT 2310
AIR FORCE GEOPHYSICS LABORATORY
HANSCOM AFB, MASSACHUSETTS 01731

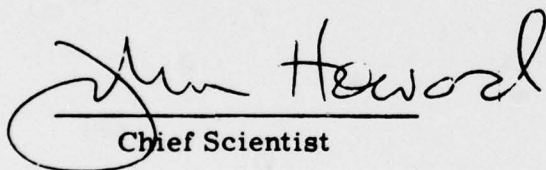
AIR FORCE SYSTEMS COMMAND, USAF



This report has been reviewed by the ESD Information Office (OI) and is releasable to the National Technical Information Service (NTIS).

This technical report has been reviewed and is approved for publication.

FOR THE COMMANDER



Chief Scientist

Qualified requestors may obtain additional copies from the Defense Documentation Center. All others should apply to the National Technical Information Service.

Unclassified

9 Instrumentation papers

SECURITY CLASSIFICATION OF THIS PAGE (When Data Entered)

REPORT DOCUMENTATION PAGE

READ INSTRUCTIONS
BEFORE COMPLETING FORM

14

1. REPORT NUMBER
AFGL-TR-77-0213, AFGL-IP-259

3. RECIPIENT'S CATALOG NUMBER

6

4. TITLE (and Subtitle)
STUDY OF THE DUAL-INPUT MODE WITH THE
AFGL TWO-METER PATH DIFFERENCE
INTERFEROMETER.

5. TYPE OF REPORT & PERIOD COVERED

Scientific Interim

10

7. AUTHOR(s)
George A. Vanasse
Hajime Sakai

6. PERFORMING ORG. REPORT NUMBER
IP No. 259

8. CONTRACT OR GRANT NUMBER(s)

9. PERFORMING ORGANIZATION NAME AND ADDRESS
Air Force Geophysics Laboratory (OP) ✓
Hanscom AFB,
Massachusetts 01731

10. PROGRAM ELEMENT, PROJECT, TASK
AREA & WORK UNIT NUMBERS

61102F
2310G101

G1

11. CONTROLLING OFFICE NAME AND ADDRESS
Air Force Geophysics Laboratory (OP)
Hanscom AFB,
Massachusetts 01731

12. REPORT DATE

4 Oct 1977

12 16p

13. NUMBER OF PAGES

14. MONITORING AGENCY NAME & ADDRESS (if different from Controlling Office)

15. SECURITY CLASS. (of this report)

Unclassified

15a. DECLASSIFICATION DOWNGRADING
SCHEDULE

16. DISTRIBUTION STATEMENT (of this Report)

Approved for public release, distribution unlimited.

DDC
RECEIVED
MAR 13 1978
B

17. DISTRIBUTION STATEMENT (of the abstract entered in Block 20, if different from Report)

18. SUPPLEMENTARY NOTES

19. KEY WORDS (Continue on reverse side if necessary and identify by block number)

Interferometry
Dual-input
Fourier spectroscopy

20. ABSTRACT (Continue on reverse side if necessary and identify by block number)

Experimental testing of the dual-input dual-output operation of the AFGL two-meter path difference interferometer is described, together with the results. It has been found that the external modulation scheme for the interferometer is poorly suited for good suppression. The reasons supporting this conclusion are presented.

1 409 578 AW

ACCESSION for	
NTIS	White Section <input checked="" type="checkbox"/>
DDC	Buff Section <input type="checkbox"/>
UNANNOUNCED	<input type="checkbox"/>
JUSTIFICATION _____	
BY _____	
DISTRIBUTION/AVAILABILITY CODES	
Dist.	AVAIL. and/or SPECIAL
A	

Contents

1. INTRODUCTION	5
2. GENERAL PRINCIPLE OF DUAL-INPUT SCHEME	6
3. DUAL-INPUT DUAL-OUTPUT	9
4. CONCLUSION	16

Illustrations

1. Cat's Eye Interferometer Showing Path of the Input Beam Striking the Upper Face of the Beamsplitter	6
2. Cat's Eye Interferometer Showing Path of the Input Beam Striking the Lower Face of the Beamsplitter	8
3. Dual-input Beam Configuration for a Roof Mirror Interferometer	9
4. Close-up View of Two-meter Path Difference Interferometer Showing the Beamsplitter and the Two Cat's Eye Assemblies	10
5. Over-all View of Interferometer Including Foreoptics	10
6. End View of Interferometer Showing the "Ways" on Which Movable Carriage is Displaced	11
7. Optical Configuration of Interferometer Set Up for Dual-Input Dual-Output Operation	12
8. Results Obtained with Setup of Figure 7	14
9. Temporal Display of the Various Detector Signals	15

Study of the Dual-Input Mode With the AFGL Two-Meter Path Difference Interferometer

1. INTRODUCTION

The technique known as background optical suppression scheme (BOSS)¹ was first conceived and suggested for military surveillance applications in September of 1975. After a preliminary crude experiment that demonstrated the validity of the concept, it was decided to support some outside effort to see just how much background suppression could be obtained. A small amount of money was obtained from the Laboratory Director's Fund for the purpose of starting a program that eventually would lead to a field demonstration of the capability of the BOSS technique. The results obtained by Visidyne Inc., the contractor, have been described in their scientific report, * and consequently will not be described here. We wish only to remark that the small breadboard interferometer built by the contractor was built for the specific purpose of background suppression. It was also decided to mount a small effort in-house of the dual-input scheme, while not impacting too much on the data-taking with the high resolving power instrument. What we report here are results and conclusions about the dual-input dual-output technique when applied to the Idealab Model 100 Interferometer at AFGL. It is a step and stop interferometer with external chopping; it was not constructed for use in a dual-input dual-output mode.

(Received for publication 30 September 1977)

1. Vanasse, G. A., and Stair, A. T. (AFGL) and Shepherd, Orr, and Reidy, W. (Visidyne) (1977) AFGL-TR-77-0135.

*In press.

2. GENERAL PRINCIPLE OF DUAL-INPUT SCHEME

Figure 1 shows the basic properties of an interferometer; this was the type used at the Air Force Geophysics Laboratory (AFGL) for Fourier spectroscopy. In Figure 1(a) the beamsplitter is shown and one path taken by part of the input beam after division at the beamsplitter. The amplitude of the input beam is A_0 , whereas a_1 and a_3 are amplitudes of the output beams generated from the single beam reflected by the upper face of the beamsplitter. (In the following, we shall not consider the reflections at the fixed and movable Michelson mirrors, but only the transmission and reflection of the beamsplitter dielectric film.) For beam a_1 we obtain as amplitude,

$$a_1 = A_0 \cdot r \cdot t, \quad (1)$$

where r and t are the amplitude reflectance and transmission, respectively.

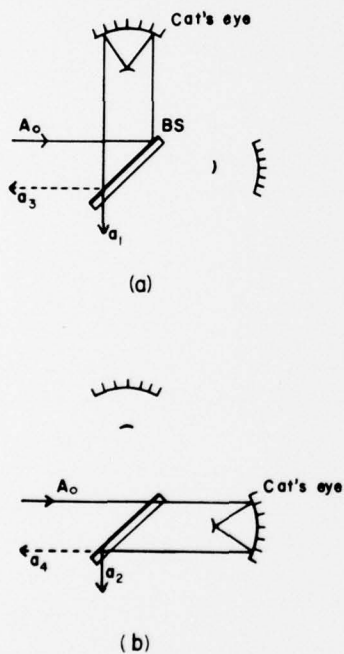


Figure 1. Cat's Eye Interferometer Showing Path of the Input Beam Striking the Upper Face of the Beamsplitter

For beam a_3 , we obtain

$$a_3 = A_0 r \cdot r = A_0 R, \quad (2)$$

where $R = r^2$ is the intensity reflection coefficient.

Figure 1(b) illustrates what happens to the beam that is first transmitted by the beamsplitter; a_2 and a_4 are the output beam amplitudes which are given by

$$a_2 = A_0 t \cdot e^{i\phi} \cdot r e^{i\pi} = -A_0 r t e^{i\phi}$$

and

$$a_4 = A_0 t \cdot e^{i\phi} t = A_0 T e^{i\phi}, \quad (3)$$

where $\phi = 2\pi\sigma\delta$, the difference in phase caused by the fact that the paths inside the interferometer differ by an optical difference of δ ; $\sigma = 1/\lambda$, the wave number of the radiation; t is the intensity transmission coefficient of the beamsplitter. The factor $e^{i\pi}$ for a_2 is due to the fact that a_2 suffers a phase change upon reflection at the film surface inside the beamsplitter substrate.

Let us now add beams a_1 and a_2 and determine the intensity I_{12} of the combined beams. We have

$$a_1 + a_2 = A_0 r t - A_0 r t e^{i\phi} = A_0 r t (1 - e^{i\phi}),$$

and

$$I_{12} = I_0 R T (1 - e^{i\phi}) (1 - e^{-i\phi}) = 2I_0 R T (1 - \cos \phi).$$

$$I_{12} = 2I_0 R T (1 - \cos \phi). \quad (4)$$

We now calculate I_{34} and obtain

$$I_{34} = I_0 (R^2 + T^2 + 2 R T \cos \phi) \quad (5)$$

$$= I_0 (R^2 + T^2) + 2I_0 R T \cos \phi$$

$$= I_0 (R+T)^2 - 2I_0 R T + 2I_0 R T \cos \phi$$

$$I_{34} = I_0 (R+T)^2 - 2I_0 R T (1 - \cos \phi). \quad (6)$$

If we assume $R + T = 1$ and add Eqs. (4) and (6) we obtain,

$$I_{12} + I_{34} = I_0, \quad (7)$$

which must be, from the conservation of energy principle. In other words, the two beams I_{12} and I_{34} produce complementary outputs as the path difference in the

interferometer is changed. It should be noted that the only assumption made was that the beamsplitter was nonabsorbing. Figure 2 illustrates the case where the input beam A_0 enters the interferometer at the bottom face of the beamsplitter. Calculation shows that the intensity due to beams a_5 and a_7 is given by

$$I_{57} = I_0(R^2 + T^2 + 2RT \cos \phi), \quad (8)$$

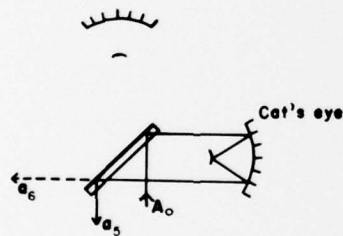
and for beams a_6 and a_8 by

$$I_{68} = 2I_0 RT(1 - \cos \phi). \quad (9)$$

The essence of the dual-beam technique is to allow two beams to enter the interferometer simultaneously via opposite faces of the beamsplitter and to let the combined beams I_{12} and I_{57} fall on one detector. The resultant intensity I_c due to the combined beams is given by

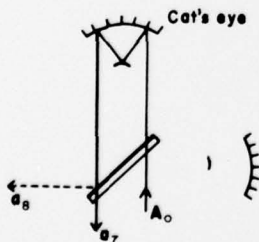
$$I_c = I_{12} + I_{57} = I_0(R+T)^2 = I_0, \quad (10)$$

a constant equal to the incoming intensity.



(a)

Figure 2. Cat's Eye Interferometer Showing Path of the Input Beam Striking the Lower Face of the Beamsplitter



(b)

3. DUAL-INPUT DUAL-OUTPUT

Figure 3 is an implementation of the technique when a roof mirror interferometer is used to obtain the optical background suppression. Figure 4 is a photograph of part of our two-meter path difference interferometer. The movable cat's eye, the perforated cylinder, can be seen at left center in the photograph; the stationary cat's eye is the cylindrical structure in the lower right of the photo. The beamsplitter, the circular looking CaF_2 plate, is mounted at an angle to, and between, the two cat's eye assemblies. All the components seen in Figure 4 are mounted on one large solid base which has its underside covered with a soft lead-vinyl material for vibration damping. Figure 5, another view of the interferometer, includes the foreoptics mounted on the separate structure seen in the upper part of the photo. It was, in part, owing to this separate cantilevered structure for the foreoptics that we were prevented from getting the suppression ratio desired, as will be explained.

Figure 6 is a full view of the instrument where the "ways" on which the movable cat's eye travels, as well as the foreoptics, can be seen. Figure 7 is a schematic of the optical setup of the system when the interferometer is used for making spectral measurements. The solid lines represent the usual arrangement for the foreoptics when operating in the single-input double-output mode. In this mode, with exception of the foreoptics, all optical components are mounted on the large interferometer base, and therefore form a very stable setup.

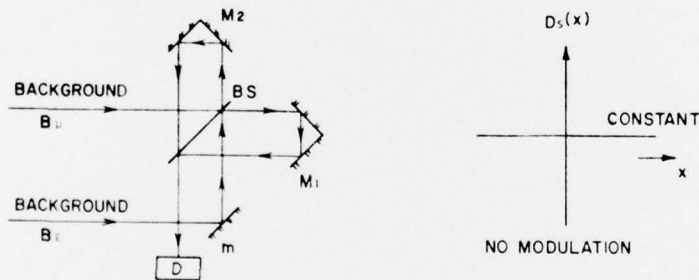


Figure 3. Dual-input Beam Configuration for a Roof Mirror Interferometer

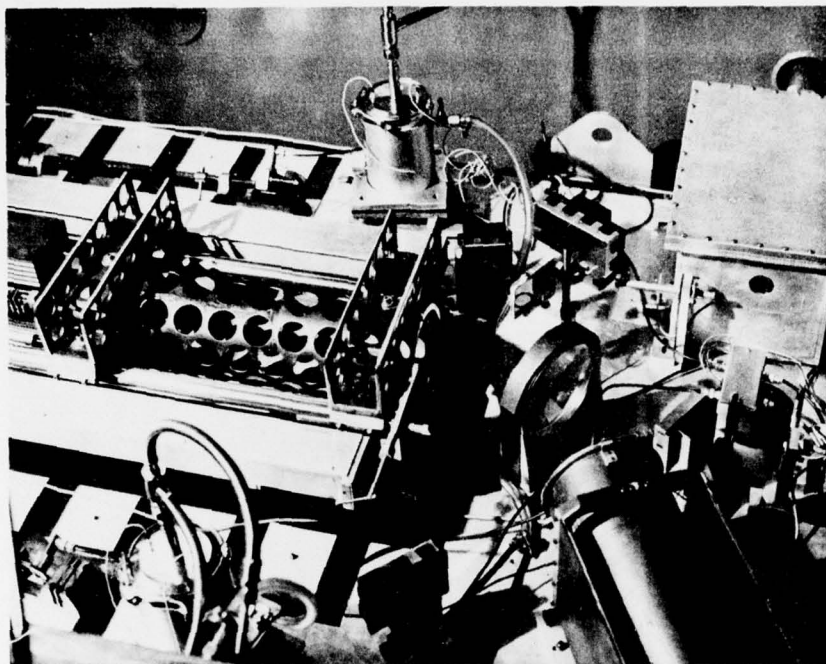


Figure 4. Close-up View of Two-meter Path Difference Interferometer Showing the Beamsplitter and the Two Cat's Eye Assemblies (see text)

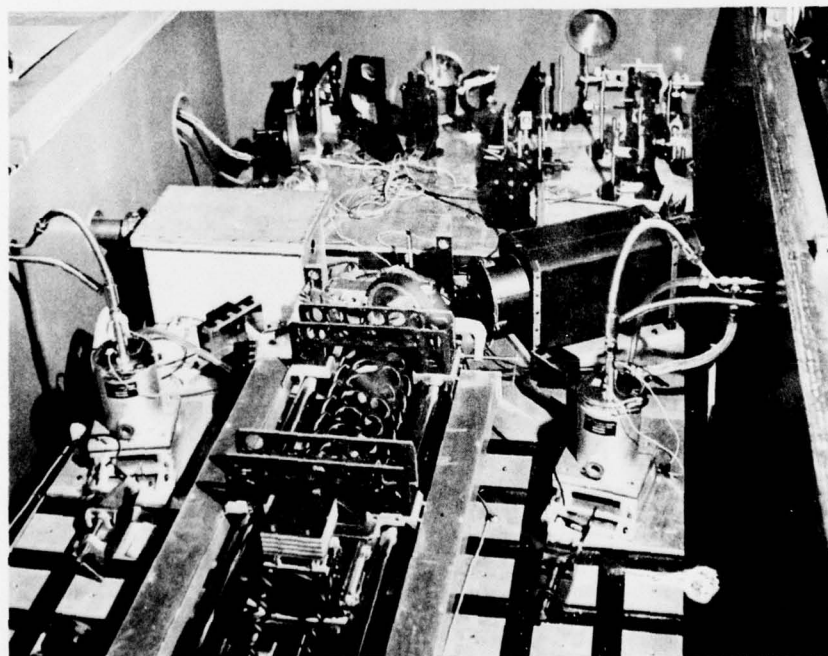


Figure 5. Over-all View of Interferometer Including Foreoptics (see text)

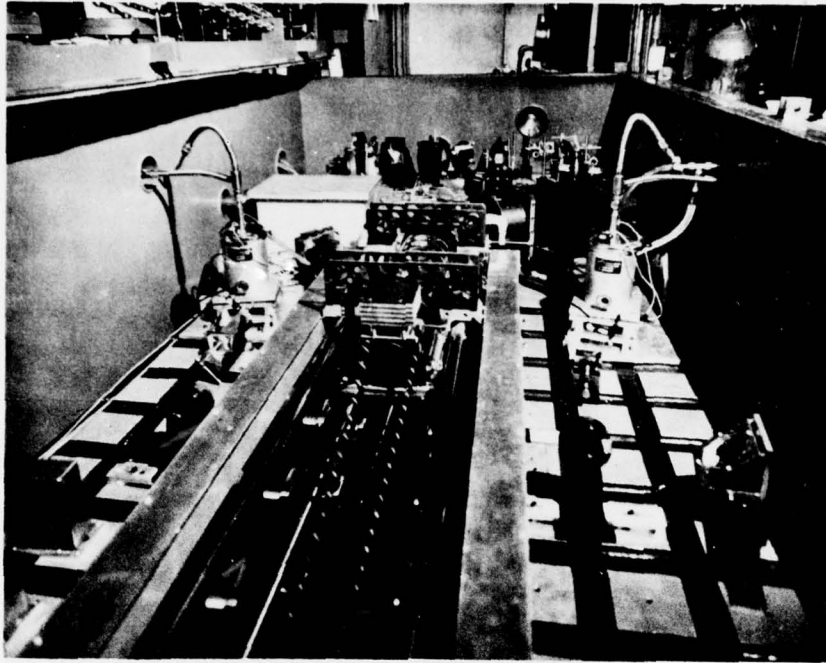


Figure 6. End View of Interferometer Showing the "Ways" on Which Movable Carriage is Displaced

The two small mirrors *m* shown dashed in Figure 7 were placed there in order to try the dual-input scheme. The source "*s*" is focused onto aperture "*a*" which has a vibrating reed chopper "*c*" placed in front of it; that is, the source radiation is externally modulated. Normally, two detectors are used and the two outputs of the interferometer are electronically differenced. This is done in an attempt to remove source fluctuations. The source radiation is chopped in order to produce a modulated intensity which then enters as collimated light into the interferometer. The outputs from the interferometer fall on separate detectors whose signals are amplified and fed into the two inputs of an operational amplifier: one to the inverted input; the other to the noninverted input. The amplifier output, considered output 1, is essentially the difference of the two detected signals. The inverted input may be considered as a separate signal which can be used to generate a synchronization pulse, whereupon both signals are then synchronously demodulated.

In the dual-input dual-output mode we should expect that the two inputs would produce complementary intensity fluctuations at each detector and therefore we should obtain a constant value plus noise from each detector; this is the ideal situation. By differencing the two detector outputs, one finds that the noise due to the source fluctuations should cancel; however, the "detector" noise should increase. The differenced signal with two detectors will then yield a gain of $\sqrt{2}$ in signal-to-noise.

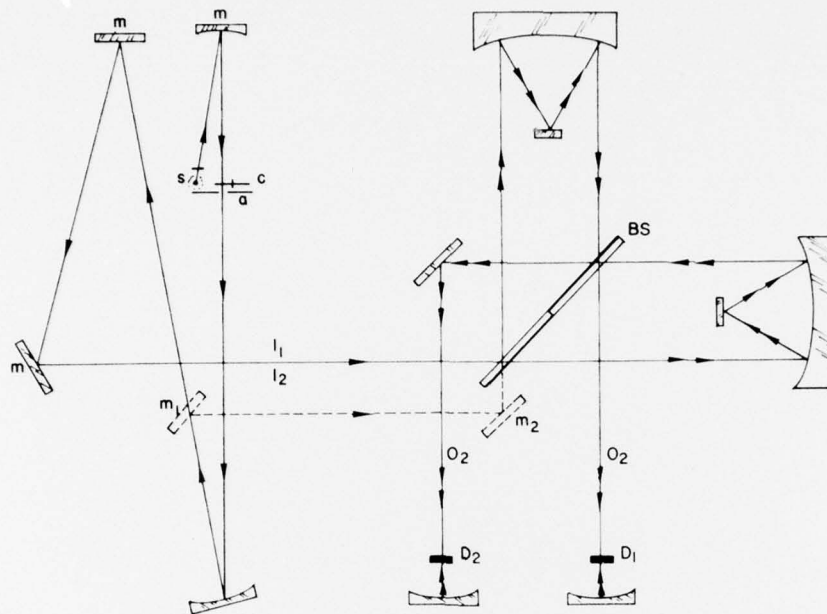


Figure 7. Optical Configuration of Interferometer Set Up for Dual-Input Dual-Output Operation. (For the interferometer, we have taken the liberty of placing the cat's eye assemblies at right angles to each other for the purpose of illustration)

Our philosophy toward trying the dual-input scheme was to preserve the present optical configuration and to implement the scheme by the addition of components that could be easily removed. In essence, we did not want the dual-input experiment to cause severe delays in returning the system to its single input operation, since, as has been shown,^{2,3,4} the instrument can yield high-quality spectra, and only in exceptional cases would the dual-input mode be necessary.

It is for this reason that we went to the configuration shown in Figure 7 where the two extra mirrors (dashed lines) allow us to obtain two inputs. The optical or electronic setup was not modified, allowing us to go to the normal mode very easily. The dual-input mode experiment was performed to gain an insight into problems associated with such a system and arrive at conclusions that would aid in choosing the type of instrument most likely to work in a field environment.

2. Sakai, H. (1974) AFCRL-TR-74-0571.
3. Sakai, H. (1976) AFGL-TR-76-0280.
4. Sakai, H., and Vanasse, G. A. (1977) AFGL-TR-77-0039.

In our experimental scheme, there were three major problems in achieving a good suppression of the interferogram modulation. These were found to be interdependent on one another in affecting the outcome. Because of this intricate interaction, the adjustments must be corrected simultaneously in order to achieve a satisfactory suppression. The application of the dual-input technique to our interferometer was much more difficult than anticipated at the outset. For a while in the course of our experiment, we were thoroughly confused with the results. Slowly we came to realize the existence of the three problems and of their intricate interaction toward the end of our experiment. What is described in the following account, records what we did and what we obtained. The first problem encountered was in trying to get the two beams of equal strengths. This we did, as best we could, by obscuring the stronger beam until the two separate interferograms looked the same near the central maximum. Beam I_2 of Figure 7 was blocked off (by masking one of the small mirrors shown dashed) and an interferogram was obtained. The mirrors were adjusted until modulation around the zero path difference was as large as we could obtain by these adjustments. Beam I_1 was then blocked off and an interferogram due to beam I_2 only was obtained and optimized by adjusting the two small mirrors shown by the dashed lines. Once the beams were of equal strength, we allowed both beams to enter the interferometer simultaneously, obtaining a combined interferogram. The results were very disappointing as the combined interferogram sometimes was even larger than the single beam interferogram. Repeating the whole procedure, we were able to obtain some suppression, though still very poor results and also a lack of reproducibility. Then we came to the conclusion that the alignment of the two input beams (which could be co-aligned inside the interferometer) was very critical and that the small mirrors (dashed in Figure 7) should be mounted more sturdily. This was easily done for mirror m_1 , but not possible for mirror m_2 (close to the beamsplitter), since there is practically no way of getting a stable mounting arrangement without the mount obscuring the many beams that traverse the area. Major modification of the optical setup would have been necessary in order to open up the space to mount mirror m_2 on a rugged base supplying what was required.

We finally came up with a cantilever arrangement which was moderately stable. The experiment was performed again, and after many attempts and much adjusting of mirrors and apertures, we obtained the result illustrated in Figure 8. The combined output is down by a factor of about 10 from the peak of input I. It was felt that we had aligned the two input beams as well as we could, considering the fact that all the foreoptics, except mirror m_2 , were mounted on a separate cantilevered base plate which, unfortunately, is subject to vibration. Nevertheless, we felt that the suppression should be better. We eventually decided to make a thorough analysis of the external modulation used in our arrangement.

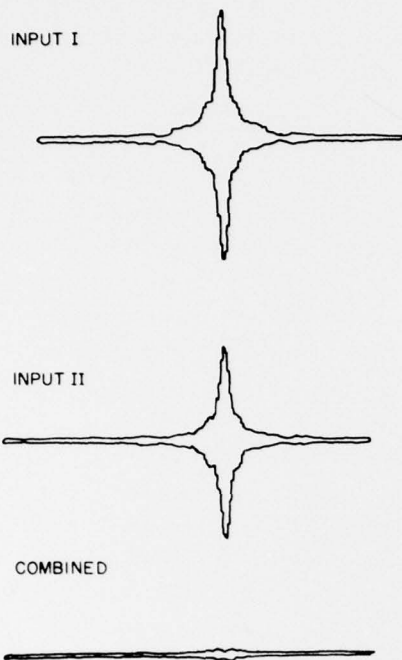


Figure 8. Results Obtained with Setup of Figure 7. The suppression is observed as the curve labeled "combined"

Since the two input beams do not follow exactly the same path to the interferometer beamsplitter, it was expected that their temporal modulation patterns generated by the chopper would be, on the whole, different. The synchronous demodulation scheme, under such a condition, exhibits a response nonlinear to the intensity level of the input signals. In Figure 9, the two beams (a) and (b) are combined to produce the beam (c), which is seen by the detector. The synchronous demodulation scheme amplifies the signal (c) with an a-c coupled amplifier, and it produces the output signal measured with respect to the average level of the signal (c). The response would become linear to both signal (a) and (b) only if their waveform takes the same pattern on the temporal scale.

In our experiment, we measured the interferogram signals produced by the individual inputs, and compared them with the dual-input signal. These interferogram signals were measured at each short time element within the chopping cycle, in order to check the linearity of response. The integrated outputs were also checked to test for any additional nonlinear behavior. To our shock we found that these time-element interferograms exhibited an extremely high degree of nonlinearity. We concluded that the nonlinear response in the synchronous demodulation scheme was definitely the factor leading to poor suppression. The second problem was further complicated by a relatively slow response of the detector with respect to

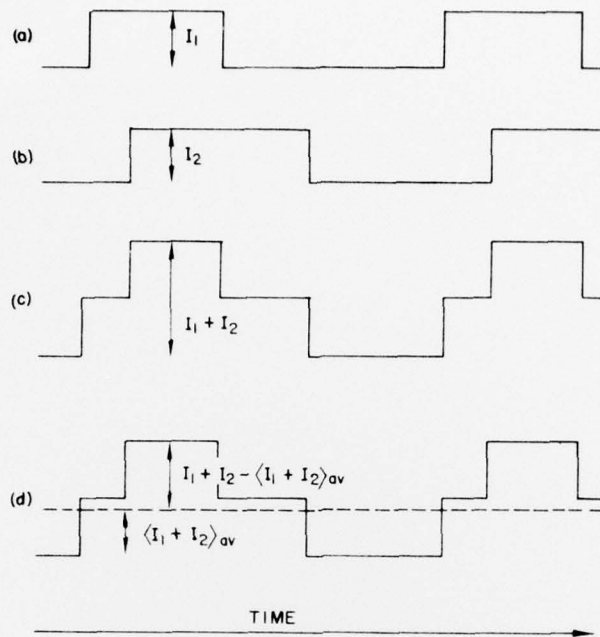


Figure 9. Temporal Display of the Various Detector Signals. Part (c) shows the sum of (a) and (b) which is seen by the detector. In (d) the electrical output is measured with respect to the average value $\langle I_1 + I_2 \rangle_{av}$

the chopping speed, as an additional phase shift was introduced to the output waveform. As we made a careful analysis of our detector electronics, we finally reached a clear understanding of why such poor results were obtained in our experiment. In using the synchronous demodulation scheme, we found that the dual-input signals must have a well-matched temporal modulation pattern in addition to the two factors that are easily recognizable: a good co-alignment and a well-matched intensity level. These three factors must be adjusted to a satisfactory degree in order to achieve good suppression. The attempt to equalize the intensity levels of both beams by adjusting the beam size affected the chopping phase. Also, this was found in the attempt to co-align both beams. The configuration used for this equipment was found inadequate for satisfaction of these three conditions simultaneously.

Either the internal modulation scheme, or the rapid scan scheme modulates the signal internally by means of the interferometer motion and produces an identical temporal response to the input beams. The problem leading to the nonlinear response is thus greatly reduced, even if not completely eliminated, because these two beams are subject to a well-matched temporal modulation.

4. CONCLUSION

It was found in this study that the alignment of the two input beams is very critical if one wishes to obtain an order of magnitude suppression or better. What has also been shown is that some form of internal chopping should be used rather than an external chopping scheme, as our system is presently set up. That is, the movable assembly is rapidly scanned such that the interferometer itself does the chopping and thereby assures that the two beams are simultaneously chopped. Also, of course, the internal modulation scheme would also work just as well, that is, assuming the beams are properly co-aligned. Also, without external chopping, a gain of a factor of 2 is realized.

It is not our intention to modify the AFGL two-meter path difference interferometer, in particular, to make it into the dual-input mode, since this would entail major modifications of our instrument, such as going to continuous rapid-scan, or some form of internal modulation. Both of these modifications would require changes in the data handling system as well. It is our judgment that if a dual-input system is needed (which is doubtful for high-resolution laboratory work), it would be better to design it for such operation at the outset.